Supporting Information for "Illuminating the pre-, co-, and post-seismic phases of the 2016 M7.8 Kaikōura earthquake with 10 years of seismicity"

C. J. Chamberlain[1], W. B. Frank[2], F. Lanza[3], J. Townend[1], E. Warren-Smith[4]

[1]School of Geography, Environment and Earth Sciences, Victoria University of Wellington, Wellington, New Zealand

[2]Department of Earth, Atmospheric and Planetary Sciences, Massachusetts Institute of Technology, Cambridge, MA, USA

[3]Swiss Seismological Service, ETH Zürich, Switzerland

[4]GNS Science, Lower Hutt, New Zealand

Contents of this file

1. Figures S1 to S9
2. Table S1

Introduction

This file contains additional figures and one table to complement the main paper. The methods used are described in the main paper with details given in figure captions.

Corresponding author: C. J. Chamberlain, School of Geography, Environment and Earth Sciences, Victoria University of Wellington, Wellington, New Zealand. calum.chamberlain@vuw.ac.nz

References

Eberhart-Phillips, D., & Bannister, S. (2015). 3-D imaging of the northern Hikurangi subduction zone, New Zealand: variations in subducted sediment, slab fluids and slow slip. *Geophysical Journal International*, *201*(2), 838–855.

Hamling, I. J., Hreinsdóttir, S., Clark, K., Elliott, J., Liang, C., Fielding, E., ... Stirling, M. (2017). Complex multifault rupture during the 2016 Mw 7.8 Kaikoura earthquake, New Zealand. *Science*, *356*(6334). Retrieved from `https://science.sciencemag.org/content/356/6334/eaam7194` doi: 10.1126/science.aam7194

Henrys, S., Eberhart-Phillips, D., Bassett, D., Sutherland, R., Okaya, D., Savage, M., ... others (2020). Upper Plate Heterogeneity Along the Southern Hikurangi Margin, New Zealand. *Geophysical Research Letters*, *47*(4), e2019GL085511.

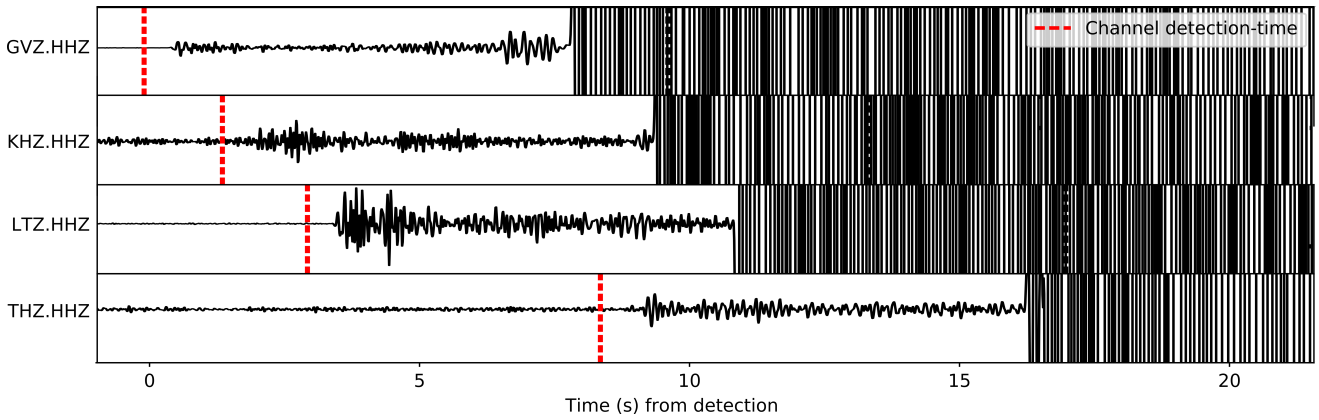

Figure S1. Waveforms of showing the P-arrivals of a foreshock 7 s prior to the Kaikōura mainshock. Red dashed lines mark the detection times (1 s before expected P-arrival) using a correlation detector with a template located (by GeoNet) at -43.63, 172.97, 15 km, within 10 km of the Kaikōura hypocentre, and within uncertainty of both locations. Clipped waveforms mark the arrival of the P-waves of the Kaikōura mainshock. Channels are labelled according the GeoNet station and channel the waveform was recorded on.

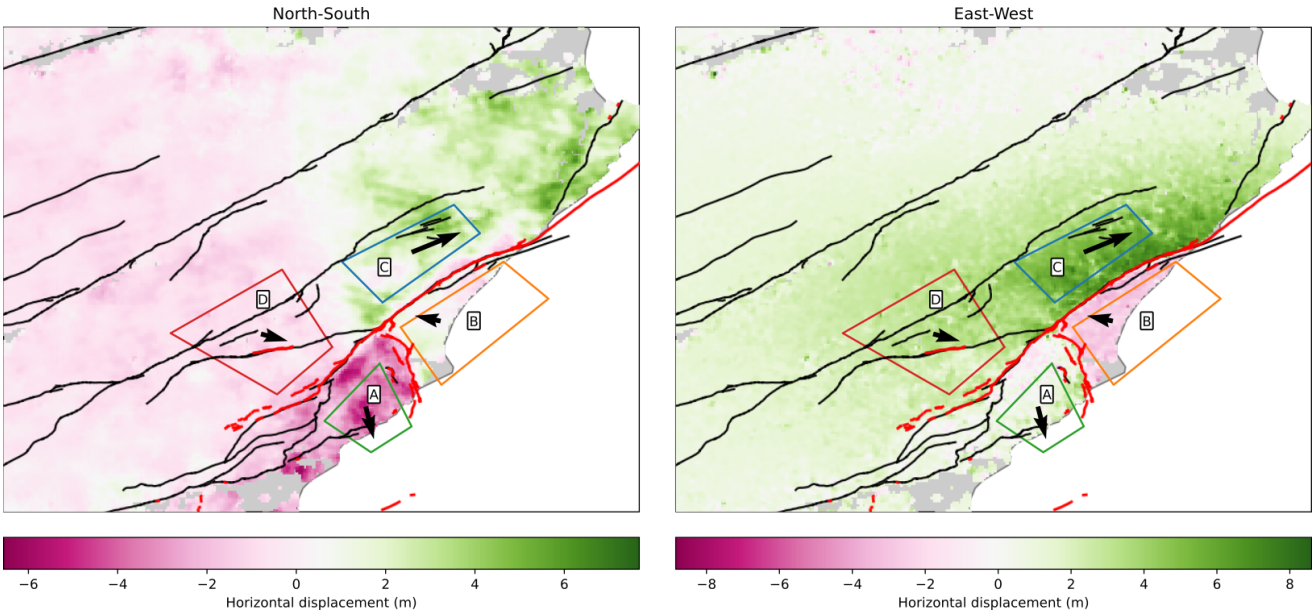

Figure S2. Horizontal InSAR derived displacement field from Hamling et al. (2017) around the Jordan Thrust-Papatea-Kekerengu-Snowgrass Creek quadruple junction. Boxes used for computing spatial average motions shown, and average displacements are plotted as arrows. These boxes were chosen to be deliberately far from the damage zone of the main faults. Colour-scales have north and east positive.

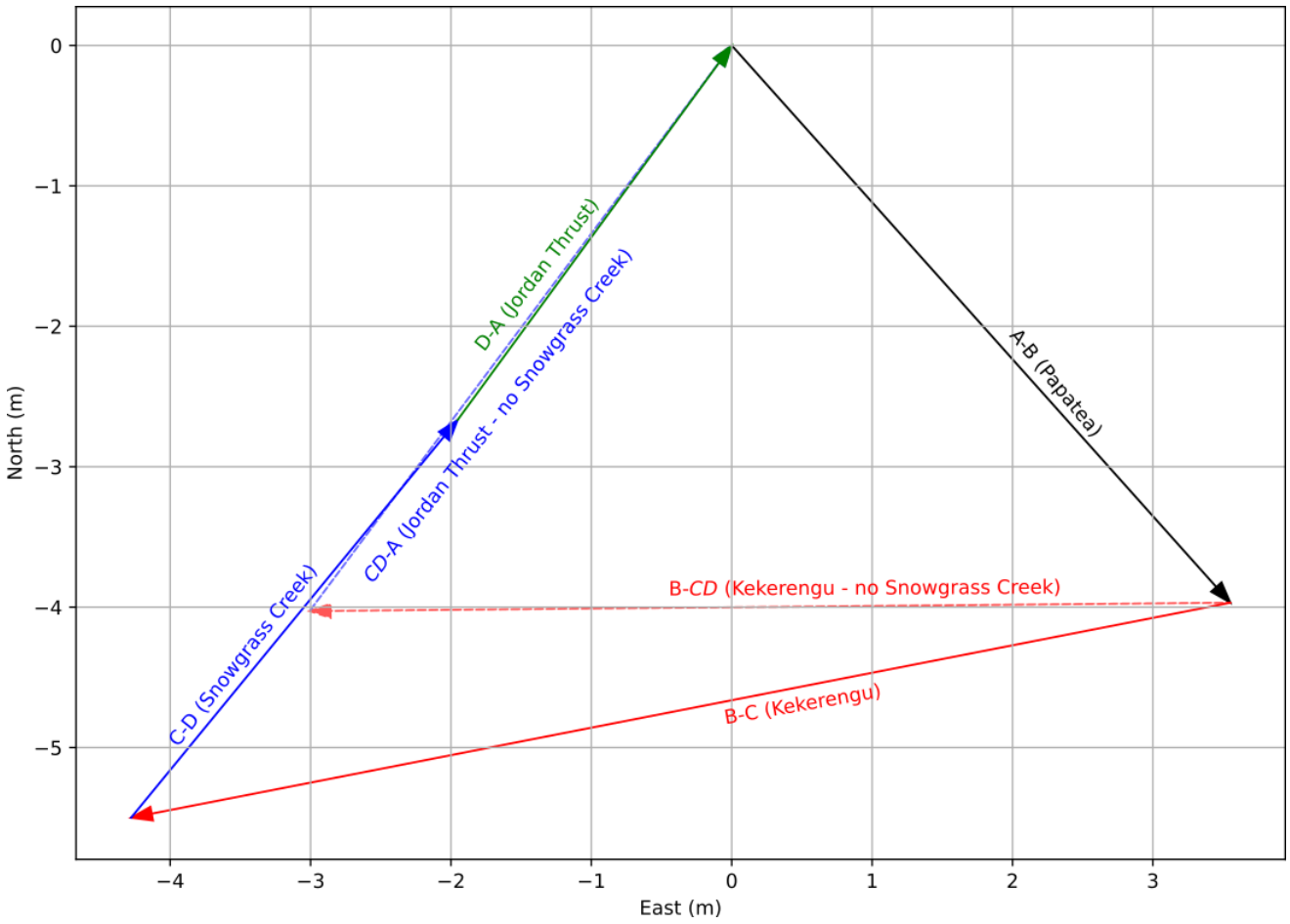

Figure S3. Circuit diagram for block motions around the Jordan Thrust-Papatea-Kekerengu-Snowgrass Creek quadruple junction. Arrows show relative motion between blocks shown in Figure S2. The dashed lines represent the same system, without the Snowgrass Creek Fault, and with motion averaged across the western side of the Jordan Thrust and Kekerengu faults.

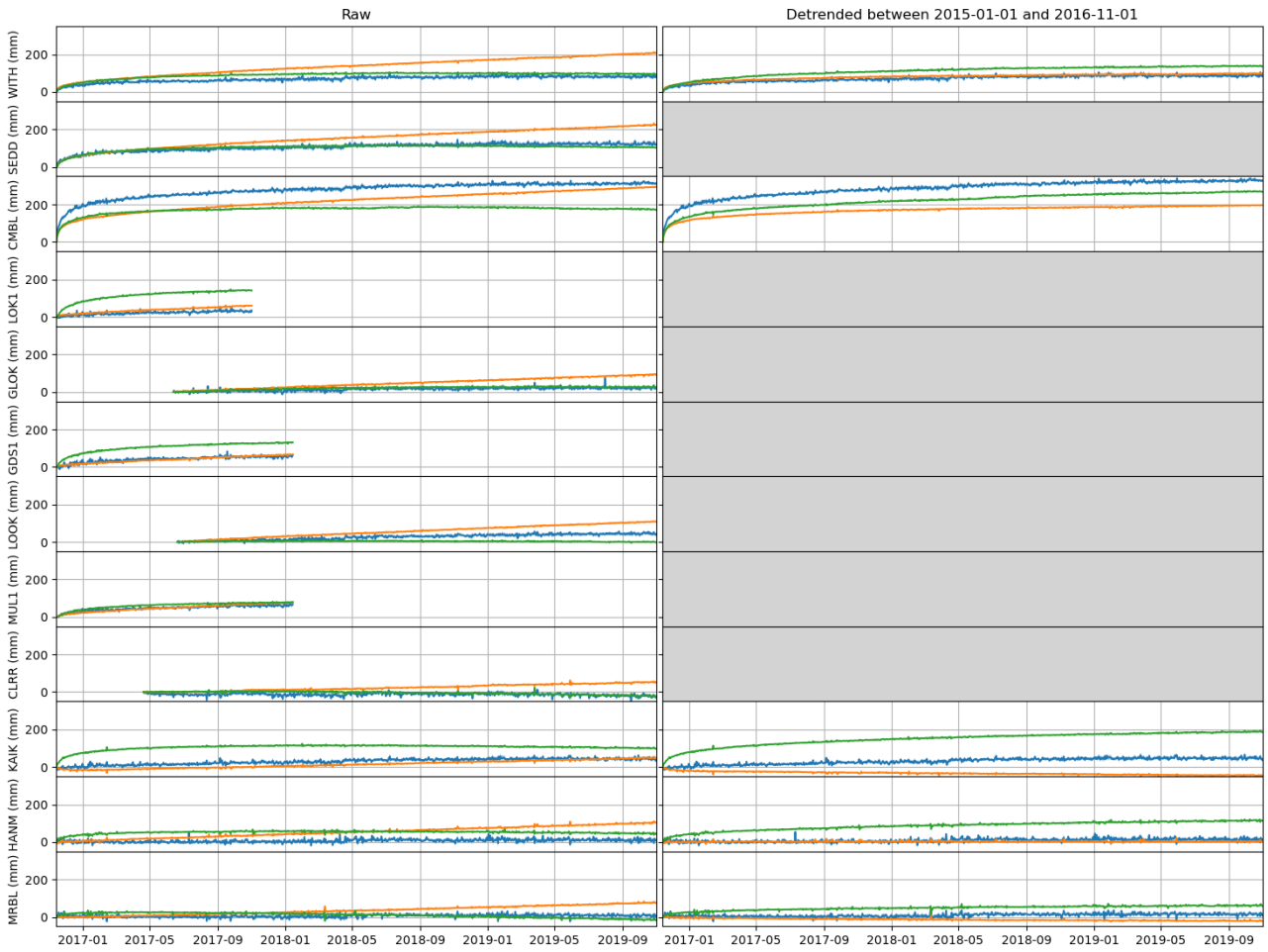

Figure S4. GPS data for all stations plotted in Fig 1. Raw left, detrended right. Blue, orange and green lines show the vertical, north and east components respectively.

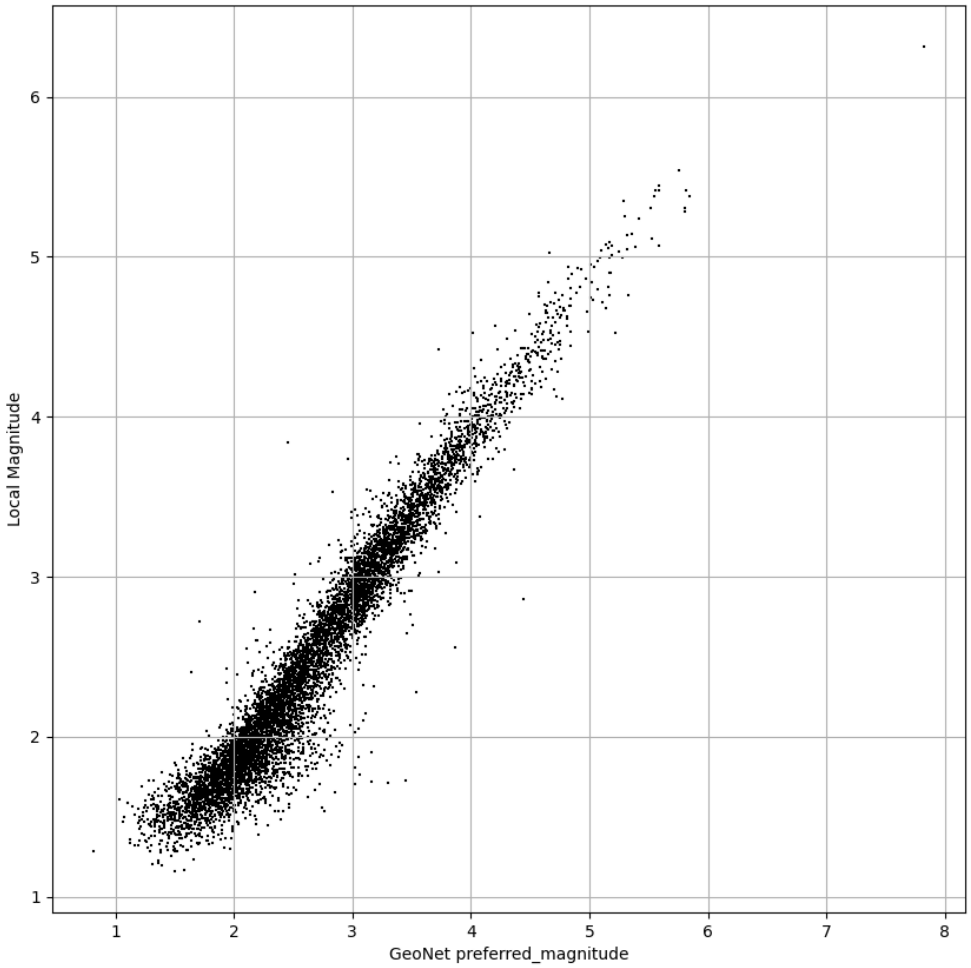

Figure S5. Comparison of Local Magnitudes (computed here) and GeoNet preferred magnitude. Note non 1:1 fit at high magnitudes as expected for the saturation of amplitude based magnitude scales. Some of the differences at low magnitudes can be attributed to significant location (and hence hypocentral distance) changes between GeoNet events and those located here, and differences in magnitudes provided by GeoNet. Note that our magnitudes are scaled to M_W, but the GeoNet comparison magnitudes are either M (summary magnitude), M_{Lv} or M_L.

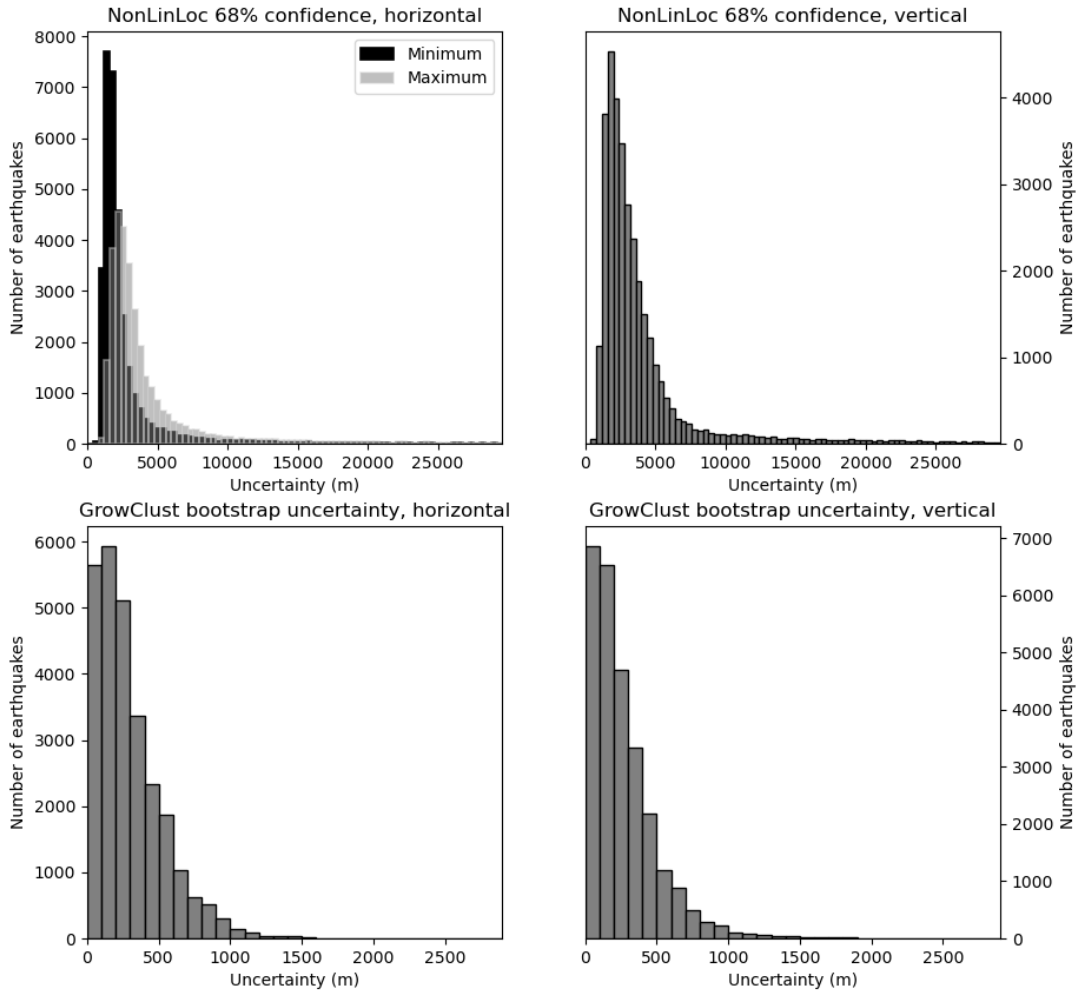

Figure S6. Horizontal and depth uncertainties for absolute (NonLinLoc, top) locations and relative relocations (GrowClust, bottom). In GrowClust, fixed locations are reported with zero uncertainty: these have been removed prior to plotting and computing the average uncertainties. The median minimum and maximum absolute horizontal uncertainties are 2.1 km and 3.7 km respectively. The median absolute depth uncertainty is 4.0 km. The median relative horizontal and depth uncertainties are both 0.4 km.

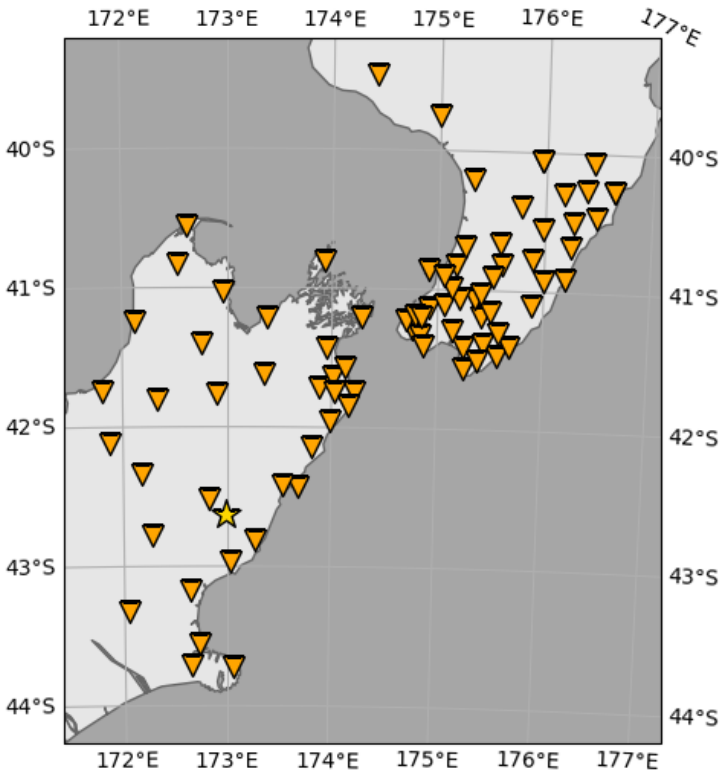

Figure S7. Stations of the STREWN and GeoNet networks (inverted triangles) used for focal mechanism inversion. Kaikōura mainshock shown as a star.

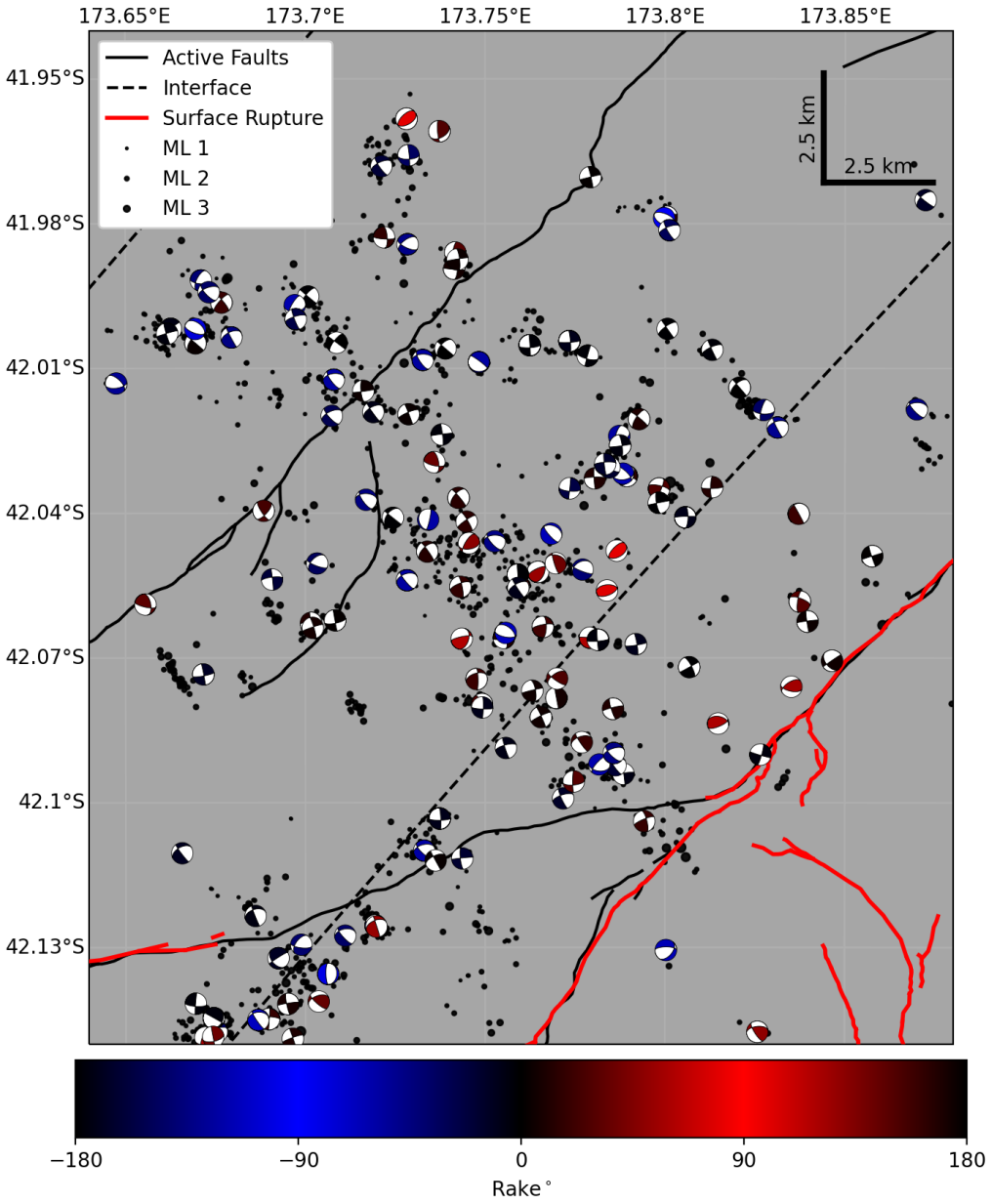

Figure S8. Focal mechanisms around the Snowgrass Creek Fault. Mechanisms are colored by rake.

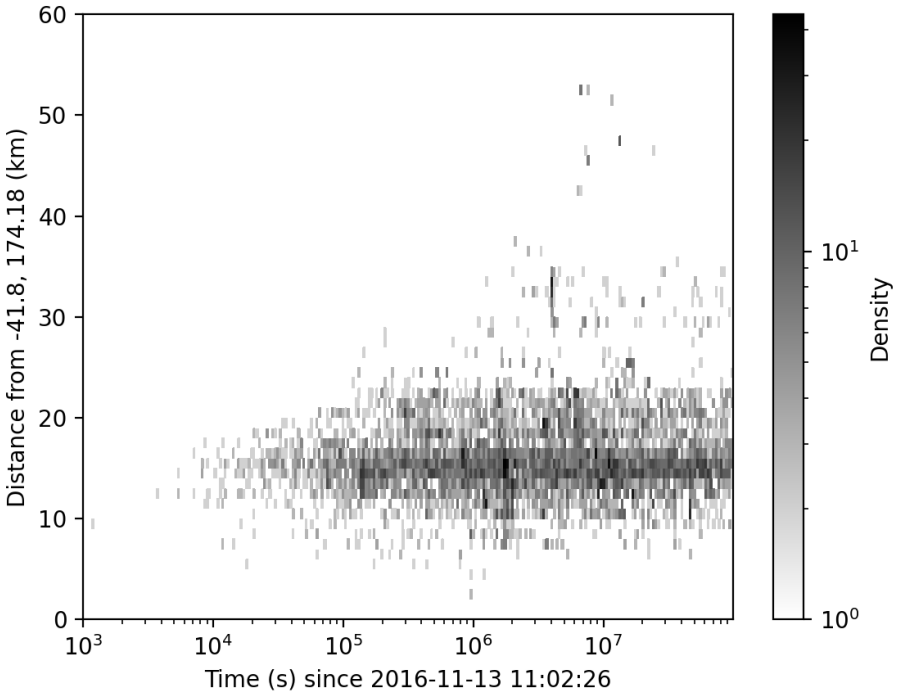

Figure S9. Earthquake density per km per log time from a point south of Cape Campbell. Only earthquakes to the NorthEast of this point are plotted. Note the clear expansion of the aftershock region with the logarithm of time.

Table S1. Velocity model used for relocation in GrowClust. Depth is to the top of the layer. Taken as the spatial average of the NZW3D 2.2 velocity model (Henrys et al., 2020) (between 72–110 km in X and -100–80 km in Y in the co-ordinate system of Eberhart-Phillips and Bannister (2015))

Depth (km)	Vp (km/s)	Vs (km/s)
-15.0	2.84	1.63
-1.0	3.67	2.09
1.0	3.94	2.26
3.0	4.29	2.47
5.0	4.69	2.71
8.0	5.24	3.01
15.0	5.78	3.27
23.0	6.61	3.73
30.0	7.33	4.15
34.0	7.82	4.47
38.0	8.21	4.73
42.0	8.35	4.80
48.0	8.41	4.88
55.0	8.42	4.88
65.0	8.44	4.88
85.0	8.35	4.83
105.0	8.38	4.84
130.0	8.41	4.87
155.0	8.34	4.82
185.0	8.42	4.87
225.0	8.56	4.95
275.0	8.67	5.01
370.0	8.88	5.13
620.0	10.20	5.90
750.0	10.60	6.13